The Addition of Water to Ethylene and *trans*-Butene Radical Cation. Model Systems for the Reaction of Alkene Radical Cations with Nucleophiles

H. Zipse

Contribution from the Institute of Organic Chemistry, TU Berlin, Str. d. 17. Juni 135, D-10623 Berlin, Germany

Received June 21, 1995[⊗]

Abstract: The reactions of one, two, or four water molecules with ethylene radical cation and the reaction of one water molecule with *trans*-2-butene radical cation have been investigated by *ab initio* calculations at the UMP2/6-31G* level. In part, PMP4/6-311+G** single point energies have been added. The reaction of one water molecule with ethylene radical cation occurs without barrier in the gas phase to form a distonic radical cation. This intermediate species reacts readily with a second water molecule to interchange water molecules through two S_N2-type reaction pathways. The influence of solvation on the substitution barrier has been studied in various ways and has been shown to increase the gas phase substitution barrier approximately twofold in water. The thermodynamic acidity of the intermediate distonic radical cation has been estimated using a thermodynamic cycle. From combined *ab initio* and solution simulation results, the acidity of the distonic ion is predicted to be somewhat smaller as compared to that of protonated ethanol. The reaction of *trans*-2-butene with water in the gas phase does not lead to the formation of a distonic radical cation. Instead, an ion−dipole complex is formed. This result is linked to the stabilization of alkene radical cations by alkyl substituents.

1. Introduction

The reaction of oxygen centered nucleophiles such as water and alcohols with alkene radical cations has attracted considerable interest over the recent years. Application of the curve crossing model by Pross[1] predicted a reaction that is slow in comparison to the reaction of nucleophiles with cations. Slow rates for the addition of methanol to radical cations of sterically congested enol ether radical cations have indeed experimentally been found by Schmittel et al.[2] Absolute rate measurements for the addition of alcohols to styrene radical cations show that alcohols react 2−3 orders of magnitude slower as compared to anionic nucleophiles such as azide anion, which reacts close to the diffusion controlled rate.[3a] This high addition rate for alcohols found in this latter study is in good agreement with earlier investigations into the addition of alcohols to radical cations of 1,1-dimethylindene and 1,1-diphenylethylene.[3b] Also, a number of cases are known, in which uncharged nitrogen centered nucleophiles react rapidly with alkene radical cations, in the gas phase as well as in solution.[4] It appears that a consistent picture concerning the addition of oxygen centered nucleophiles to alkene radical cations cannot be given at the moment since examples for both fast and slow addition processes exist. Most experimental and theoretical investigations concentrate on the initial addition step. Very little is known about the fate of the radicals created in this initial step. What is the barrier of the initial addition step? Which reaction pathways exist between the adduct radical cation and reaction products? How facile does deprotonation occur? In order to answer these general questions about the reaction mechanism, we have investigated two small model systems: the reaction of water with ethylene radical cation and with *trans*-2-butene radical cation.

2. Theoretical Methods

Geometry optimizations were all performed at the UMP2 level of theory using the 6-31G* split valence basis set. Single point calculations on stationary points were performed up to the UMP4 level of theory with the extended 6-311+G** basis set. Since the amount of spin contamination varies somewhat between the different structures, the largest spin contaminant has been projected out using Schlegel's method and the resulting spin-projected MP4 energies (PMP4) used to compare the relative energies of stationary points. Core electrons were kept frozen in all post Hartree−Fock calculations. All *ab initio* calculations were performed using GAUSSIAN 92, Rev. C.[5] All Monte Carlo solution simulations have been performed with the program BOSS, version 3.4.[6]

3. Water as a Substrate—the Gas Phase Situation

3.a. The Water + Ethylene Radical Cation System. The gas phase potential energy surface for the water + ethylene system has first been investigated by Golding et al. at the Hartree−Fock level using UHF/4-31G energies on UHF/STO-3G optimized structures.[7] A refined investigation at higher theoretical level was later published by Bouma et al., in which UHF/4-31G optimized geometries have been combined with

[⊗] Abstract published in *Advance ACS Abstracts,* November 15, 1995.

(1) (a) Pross, A. *J. Am. Chem. Soc.* **1986**, *110*, 3537. (b) Shaik, S. S.; Pross, A. *J. Am. Chem. Soc.* **1989**, *111*, 4306.

(2) Schmittel, M.; Röck, M. *Chem. Ber.* **1992**, *125*, 1611.

(3) (a) Workentin, M. S.; Schepp, N. P.; Johnston, L. J.; Wayner, D. D. M. *J. Am. Chem. Soc.* **1994**, *116*, 1142. (b) Mattes, S. L.; Farid, S. *J. Am. Chem. Soc.* **1982**, *104*, 1454. Mattes, S. L.; Farid, S. *J. Am. Chem. Soc.* **1986**, *108*, 7356.

(4) (a) Heinrich, N.; Koch, W.; Morrow, J. C.; Schwarz, H. *J. Am. Chem. Soc.* **1988**, *110*, 6332. (b) Drewello, T.; Heinrich, N.; Maas, W. P. M.; Nibbering, N. M. M.; Weiske, T.; Schwarz *J. Am. Chem. Soc.* **1987**, *109*, 4810. (c) H. Parker, V. D.; Tilset, M. *J. Am. Chem. Soc.* **1987**, *109*, 2521.

(5) Frisch, M. J.; Trucks, G. W.; Schlegel, H. B.; Gill, P. M. W.; Johnson, B. G.; Wong, M. W.; Foresman, J. B.; Robb, M. A.; Head-Gordon, M.; Replogle, E. S.; Gomperts, R.; Andres, J. L.; Raghavachari, K.; Binkley, J. S.; Gonzalez, C.; Martin, R. L.; Fox, D. J.; DeFrees, D. J.; Baker, J.; Stewart, J. J. P.; Pople, J. A. GAUSIAN92/DFT, Revision F.2, Gaussian, Inc.; Pittsburgh, PA, 1995.

(6) Jorgensen, W. L. BOSS, Version 3.4; Yale University; New Haven, CT, 1992.

(7) Golding, B. T.; Radom, L. *J. Am. Chem. Soc.* **1976**, *98*, 6331.

0002-7863/95/1517-11798$09.00/0

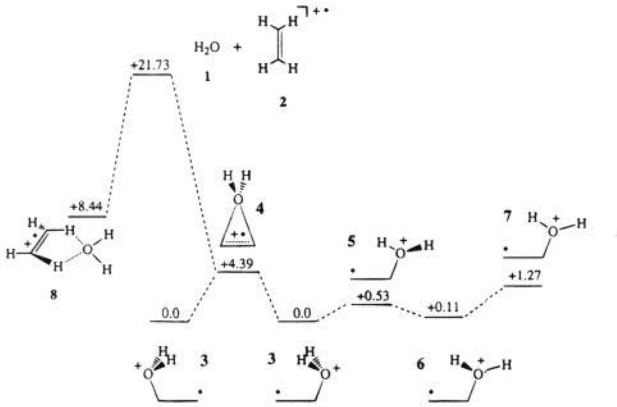

Figure 1. Gas phase potential energy surface for the addition of water to ethylene radical cation at the PMP4/6-311+G**//UMP2/6-31G* + ΔZPE(UMP2/6-31G*) level of theory.

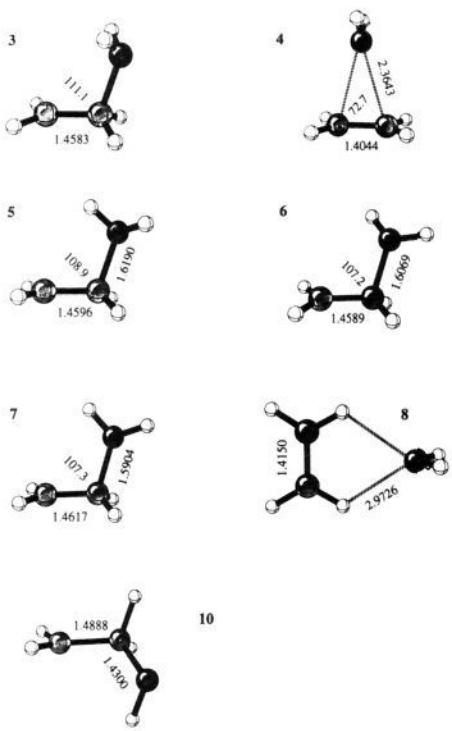

Figure 2. UMP2/6-31G* optimized geometries of stationary points on the water + ethylene radical cation potential energy surface and of ethanol-1-yl radical.

UHF/6-31G** and MP3/6-31G single point energies to construct "MP3/6-31G**" relative energies using the additivity approximation.[8] The most recent treatmentt by Postma et al. also makes use of the additivity scheme combining SDCI/4-31G and UHF/6-31G** energies on UHF/4-31G geometries. This work also includes results from mass spectrometric measurements.[9] Our PMP4/6-311+G**//UMP2/6-31G* results are in full agreement with the results obtained in the latter two studies. Figure 1 shows a schematic view of the potential energy surface with its most relevant structures, which are also shown in Figure 2 as three-dimensional plots. Absolute and relative energies are given in Table 1. Generally, the essential features of the potential energy surface are well described already at the PMP2/6-31G* level of theory. Inclusion of differences in zero point

(8) Bouma, W. J.; Nobes, R. H.; Radom, L. *J. Am. Chem. Soc.* **1983**, *105*, 1743.

(9) Postma, R.; Ruttink, P. J. A.; Van Baar, B.; Terlouw, J. K.; Holmes, J. L.; Burgers, P. C. *Chem. Phys. Lett.* **1986**, *123*, 409.

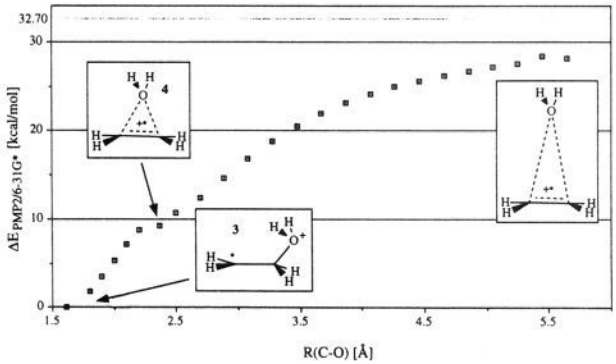

Figure 3. Potential energy curve for water addition to the ethylene radical cation at the PMP2/6-31G*//UMP2/6-31G* level of theory.

vibrational energy reduces relative energies between stationary points by as much as 4.9 kcal/mol. Single point calculations with the larger 6-311+G** basis set diminish the energy differences between all stationary points even further. Increasing perturbation order from MP2 to MP4(SDTQ) has, on comparison, only a small influence.

Addition of water to ethylene radical cation leads to distonic ion **3** as the most stable adduct. The water molecule in **3** is bound only weakly and can move from one end of the ethylene moiety to the other through low lying transition structure **4**. Symmetric structure **4** is not a minimum at any of the theoretical levels investigated here, even though the energy difference relative to **3** is decreasing steadily with increasing theoretical level. Rotation around the carbon oxygen bond in **3** leads to a second conformer **6** of almost identical energy. The only significant difference between UHF/4-31G and UMP2/6-31G* optimized geometries occurs in complex **8**, which is located +8.4 kcal/mol above distonic ion **3**. While UHF/4-31G optimization finds coordination by only one of the ethylene hydrogen atoms, UMP2/6-31G* optimization leads to the bifurcated orientation as shown in Figure 2. The most interesting question was, however, in how far the barrier height for the water−ethylene radical cation addition process can be determined. As transition state searches from a variety of starting geometries were unsuccessful, the minimum energy reaction path was investigated starting from distonic ion **3** by stepwise increasing the carbon oxygen bond distance. The resulting PMP2/6-31* potential energy curve is given in Figure 3. As the carbon−oxygen bond distance is enlarged, the O−C−C bond angle becomes smaller until symmetric structure **4** is reached at around 2.4 Å. Further stretching of the carbon−water bond distance up to ca. 5.5 Å leads to a steady increase in potential energy without ever reaching a maximum along the pathway. Even at a distance of 5.5 Å, the energy of the system remains significantly below the energy of the separate reactants of +32.7 kcal/mol at the PMP2/6-31G*//UMP2/6-31G* level of theory. One can therefore conclude at this point that the addition of water to ethylene appears to occur without barrier in the gas phase.

3.b. The 2*Water + Ethylene Radical Cation System. This system has recently been investigated through ICR experiments and been compared to the reaction of water with protonated ethanol.[10] In this study it was observed that protonated ethanol and water exchange protons in a stepwise fashion, while reaction with ^{18}O-labeled water did not lead to incorporation of ^{18}O into protonated ethanol. Distonic ion **3**, in contrast, does not show stepwise exchange of protons, but shows incorporation of ^{18}O when reacted with ^{18}O-labeled water.

(10) Stirk, K. G.; Kenttämaa, H. I. J. *Chem. Phys.* **1992**, *96*, 5272.

Table 1. Absolute and Relative Energies and Zero Point Vibrational Energies for Stationary Points on the Water + Ethylene Radical Cation and the Water + *trans*-2-Butene Radical Cation Potential Energy Surface[g]

structure	E_{tot}[a] (PMP2/6-31G*)	E_{tot}[a] (PMP2/6-311+G**)	E_{tot}[a] (PMP4/6-311+G**)	ZPE[b]	NIMAG[c]	ΔE_1[d]	ΔE_2[e]	ΔE_3[f]
1 + 2	−154.11534	−154.24201	−154.29264	45.0	0	+32.7	+22.3	+21.7
3	−154.16764	−154.28538	−154.33516	49.9	0	0.0	0.0	0.0
4	−154.15129	−154.27354	−154.32462	47.7	1	+10.3	+5.2	+4.4
5	−154.16576	−154.28400	−154.33377	49.6	1	+1.0	+0.6	+0.5
6	−154.16693	−154.28522	−154.33490	49.9	0	+0.3	+0.1	+0.1
7	−154.16233	−154.28168	−154.33103	48.6	1	+3.2	+1.0	+1.3
8	−154.14346	−154.26650	−154.31705	47.0	0	+15.0	+8.9	+8.4
1 + 25	−232.50164	−232.68681		81.4	0	+15.7	+11.8	
26	−232.52662	−232.70887		83.4	0	0.0	0.0	
27	−232.52659	−232.70896		83.3	1	+0.02	−0.16	
28	−232.52181					+3.0		

[a] UMP2/6-31G* optimized geometries. [b] Unscaled UMP2/6-31G* vibrational frequencies. [c] Number of imaginary frequencies. [d] PMP2/6-31G*//UMP2/6-31G* energies. [e] PMP2/6-311+G**//UMP2/6-31G* energies + ΔZPE(UMP2/6-31G*). [f] PMP4/6-311+G**//UMP2/6-31G* energies + ΔZPE(UMP2/6-31G*). [g] Absolute energies are in hartrees and relative energies in kcal/mol.

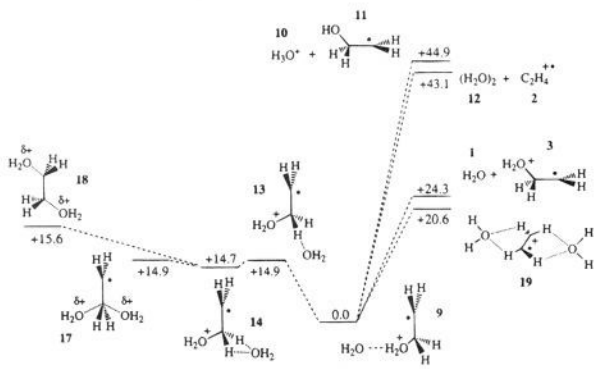

Figure 4. Stationary points on the gas phase potential energy surface for the addition of water to distonic ion **1** (not drawn to scale). Relative energies are given at the PMP4(SDTQ,FC)/6-311+G**//UMP2/6-31G* + ΔZPE(UMP2/6-31G*) level of theory.

Scheme 1

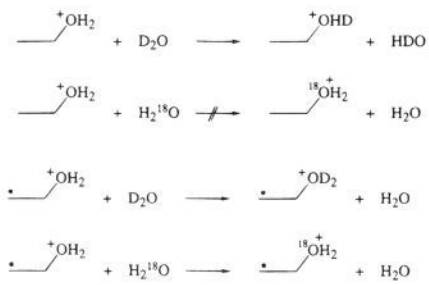

This was interpreted as a facile replacement of the water molecule in distonic ion **3** by a second water molecule. The mechanism was expected most likely to involve "an electrostatically bound ion−dipole complex of water and ionized ethylene." Even without predicting an exact mechanism, this experimental result sets an upper limit for the barrier of water exchange in distonic ion **3**, which has to be lower than the entry channel to be observable in ICR experiments.

The most relevant parts of the potential energy surface for water + distonic ion **3** have again been studied at the PMP4/6-311+G**//UMP2/6-31G* level of theory (Figure 4 and 5). The most stable structure in this part of the PES is the hydrogen-bonded complex **9**, which is 24.3 kcal/mol more stable as compared to the separate reactants. This large value reflects considerable structural relaxation of the distonic ion moiety in **9**. The C−O bond in **9** is much shorter (1.54 Å) as compared to the same bond in **3** (1.61 Å). Comparing the bond energy of 43.1 kcal/mol between the water dimer and **2** with the corresponding value of 21.7 kcal/mol for the addition of water

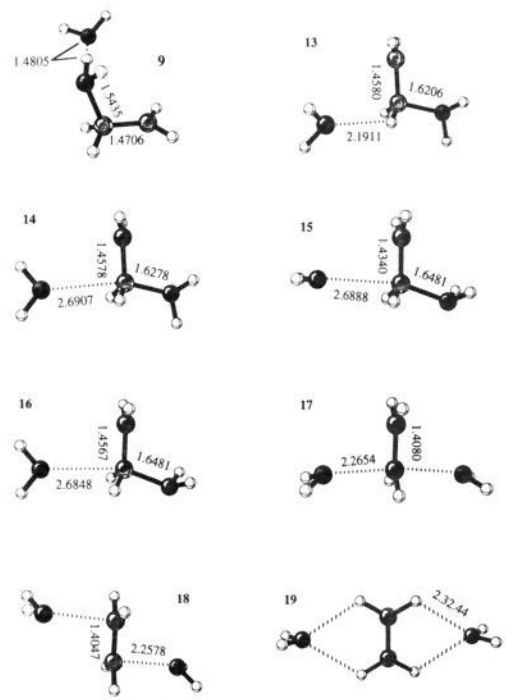

Figure 5. Structures of stationary points on the $2H_2O$ + ethylene radical cation potential energy surface (UMP2/6-31G*).

to **2**, the C−O bond strength effectively doubles through inclusion of a second water molecule. This increased bond strength results from the enhanced nucleophilicity of the water dimer as compared to a single water molecule toward the ethylene radical cation.

The acidity of **9** can be estimated by calculation of the energy of dissociation into H_3O^+ and ethanol-1-yl radical (**11**). No complex could be found for these two species, since proton transfer and formation of complex **9** appears to occur without significant barrier. From the energy difference of +44.9 kcal/mol, it is obvious that **11** is much more basic as compared to water and distonic ion **3** consequently much less acidic as compared to the hydronium ion. There is, however, no large difference between the gas phase acidity of **3** and protonated ethanol.[11] Surprisingly, the reaction energy between the initial stage (water dimer + ethylene radical cation) and the separate hydronium ion + ethanol radical **11** is positive! That is, even though there is no barrier for any of the intermediate steps, the

(11) Raghavachari, K.; Chandrasekhar, J.; Burnier, R. C. *J. Am. Chem. Soc.* **1984**, *106*, 3124.

reaction will not be efficient in the gas phase since the reaction is thermodynamically unfavorable. Even if one considers the two water molecules to react separately and not as a water dimer, the reaction would be exothermic by only 1.1 kcal/mol! In solution, the exothermicity will, of course, be strongly influenced by solvent effects. This is especially true for the current system, as any kind of polar solvent will strongly solvate the hydronium ion, while the stabilization of ethylene radical cation cannot be predicted so easily.

Besides complex **9**, a second complex **14** exists, in which the water molecule is attached to the "backside" of **3**. This second complex can be reached from **9** through transition structure **13**, which is energetically and structurally very similar to **14**. Rotation around the C−O bonds in complex **14** leads to isomers **15** and **16** (Figure 5). In all three complexes the two water molecules are properly positioned for nucleophilic S_N2-type exchange processes. It is only from complex **14**, however, that the transition structure for such a process **17** can be reached, since rotation around the C−O bonds in **15** and **16** occurs well before reaching a transition structure for water exchange. Normal mode analysis for **17** shows only one negative frequency of -134 cm^{-1}. The vanishingly small substitution barrier of +0.2 kcal/mol for this $S_{RN}2$ process results from a low electronic barrier of +1.9 kcal/mol and a zero point energy correction of −1.7 kcal/mol. Considering the very small energy difference between **13**, **14**, and **17** and the large variations of barriers in reactions of radical ions with level of theory,[12] one has to conclude that exchange of water starting from **13** through **14** and **17** faces practically no barrier. This value has to be compared with the corresponding barrier in the closed shell system, which has been calculated to +11.0 kcal/mol at the HF/6-31G**//HF/3-21G level for the S_N^2-reaction of water with protonated ethanol. Since inclusion of electron correlation effects significantly alters activation barriers, the barrier in the closed shell system should be compared with the UHF/6-31G**//UHF/3-21G barrier in the open shell system. Without zero point correction this barrier amounts to +2.47 kcal/mol for the reaction of **14** to **17**. Thus, the barrier for the S_N2-substitution process of water with protonated alcohols is lowered by 8.5 kcal/mol once a radical center has been introduced adjacent to the reaction center! It is also noteworthy that this effect is purely intrinsic, as the strength of ion−dipole complexes is of rather similar magnitude in open and closed shell cases. This "$S_{RN}2$" reaction path has also been found in *anionic* systems, where the barrier is lowered by ca. 11 kal/mol through introduction of a neighboring radical center.[12]

Water exchange in complex **14** can also occur through structure **18**, in which the loosely bound water molecule attacks the radical center. As the new C−O bond is formed, the adjacent C−O bond is cleaved leaving the radical center behind instead. This "$S_{RN}2'$-pathway" has also been found in anionic radicals, where it is even more facile than the already favorable direct $S_{RN}2$ displacement.[13] Structure **18** is not a genuine transition structure as frequency calculations only show positive vibrational frequencies. The origin of the problem can be detected in Figure 6, in which potential energy curves leading from **14** to either **17** or **18** are compared. While the reaction from **14** through **17** yields a smooth, steady potential energy curve, a sudden step is found just before reaching the expected transition structure **18**. This discontinuity has been a frequent problem in calculations on open shell substitution processes based on monodeterminental wave functions and results from insufficient mixing of the contributing electronic states.[13,14]

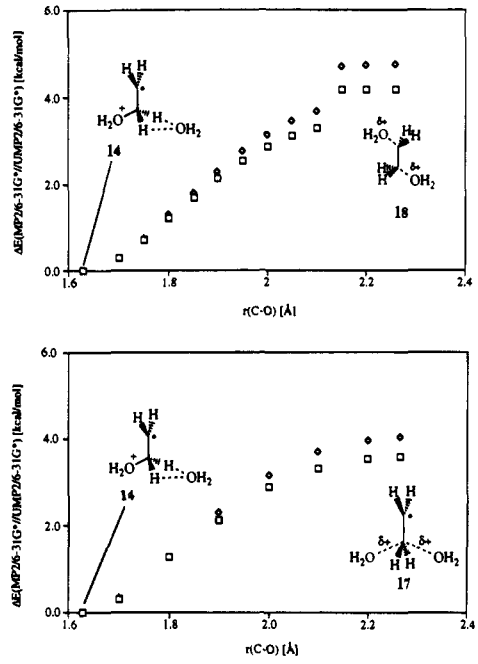

Figure 6. Potential energy profiles for the $S_{RN}2$- (lower curve) and $S_{RN}2'$- (upper curve) substitution reactions of the water + distonic radical cation system. Values at the UMP2/6-31G* level (open diamonds) and PMP2/6-31G* level (open boxes) are shown.

Despite these methodological problems, the barriers for water exchange through either $S_{RN}2$ or $S_{RN}2'$ pathways are similar at various levels of theory and are always well below the energy of the separate reactants.

The low barriers found for the "S_N2" analogous reaction pathways of course lead to the question, whether competing "S_N1" versions exist, which also benefit from the open shell character of distonic ion **3**. Clearly, the dissociation of complex **9** into the water dimer **12** and ethylene radical cation **2** is very unfavorable as all complexation energy due to the formation of an ion−dipole complex is lost. This is not the case in complex **19**, in which no C−O bonds exist, but which is stabilized by attractive ion−dipole forces. Since complex **19** is located 3.6 kcal/mol *below* the combined energies of distonic ion **3** and water, exchange of the water molecule in **3** through complex **19** should be observable in ICR experiments. Still, the exchange through the S_N2-type pathways discussed before is significantly more facile with barriers at least 5.0 kcal/mol lower than complex **19**.

4. Solvent Induced Changes

The question remains, whether the stationary points found on the $2*H_2O + C_2H_4^{\bullet+}$ potential energy surface will be significantly altered upon complete solvation with water or other polar solvents. Certainly, the difference between complexes **9** and **14** will vanish, since the two different coordination sites occupied by water molecules in these complexes will then be occupied simultaneously by separate water molecules. The most relevant questions for understanding the reactivity observed in the reactions of alkene radical cations with water are those of the barrier heights for $S_{RN}2$- and $S_{RN}2'$-reactions and the question of the acidity of distonic ion **3** in solution.

4.a. The $S_{RN}2$-Barrier Height in Solution. Even though a complete answer will only be available from full quantum mechanical fluid dynamics simulations, we have made an attempt to estimate solvation effects on the **14/17** interconversion barrier by three different approaches. First, monosolvation

(12) Zipse, H. *Angew. Chem., Int. Ed. Engl.* **1994**, *33*, 1985.
(13) Zipse, H. *J. Am. Chem. Soc.* **1994**, *116*, 10773.
(14) Fox, G. L.; Schlegel, H. B. *J. Am. Chem. Soc.* **1993**, *115*, 6870.

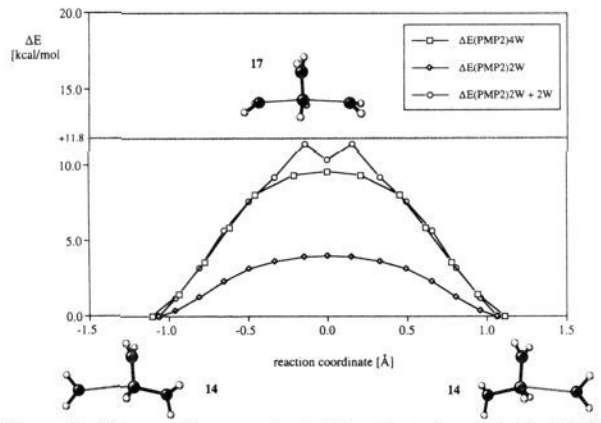

Figure 7. Solvent effects on the $S_{RN}2$-barrier at the *ab initio* PMP2/6-31G* level.

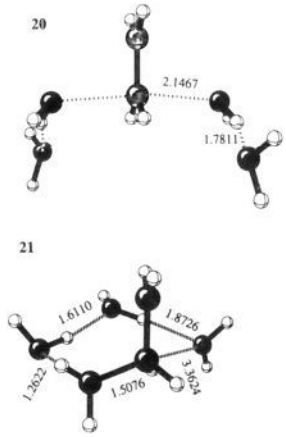

Figure 8. UMP2/6-31G* structures of stationary points in the model system containing four water molecules.

energies were calculated at the UMP2/6-31G* level of theory for all those points along the reaction coordinate that are shown in Figure 6. Structures **14** and **17** and a number of intermediate points were held rigid at the UMP2/6-31G* geometries. The additional water molecule included as a probe for solvent interactions was held rigid at the TIP4P geometry also employed in Monte Carlo simulations.[12] Only the intermolecular degrees of freedom were optimized at the UMP2/6-31G* level of theory. For each point along the reaction coordinate **14/17**, a number of different orientations exist for monosolvation. The most relevant structures are those, in which the additional water molecule coordinates either to the strongly bound or to the loosely bound water molecules in **14**. PMP2/6-31G* interaction energies for both orientations were added to the gas phase potential energy of the uncomplexed structure and a new potential energy curve results, which now includes interactions with two "nonsimultaneously" solvating water molecules. The resulting curve "ΔE(PMP2) 2W + 2W" is shown in Figure 7, which also includes the unchanged PMP2/6-31G* curve connecting **14** and **17** (designated "ΔE(PMP2) 2W"). Energies given are relative to the separate reactants water and distonic ion **3**. Treatment of solvent effects in this way increases the barrier for $S_{RN}2$-substitution by +7.4 kcal/mol. The potential energy curve also develops a shallow minimum at the top, transforming the former transition structure **17** into a high energy intermediate. In how far is the shape and the height of the new potential energy curve due to restricted geometry optimizations or other simplifications in this "solvation model"? This question can partially be answered by full relaxation of all geometric variables besides the one defining the reaction coordinate. To also eliminate artifacts due to the presence of only one solvating water molecule at a time, the potential energy curve for the interconversion of **14** through **17** was reoptimized with two additional water molecules at the PMP2/6-31G*//UMP2/6-31G* level of theory ("ΔE(PMP2) 4W" in Figure 7). The new transition structure **20** (Figure 8) has two water molecules attached at either side of the ethylene radical cation moiety. The breaking/forming C−O bonds are slightly shorter in **20** as compared to **17**. This is well in line with the enhanced nucleophilicity of the water dimer as compared to single water molecules noted before. Structure **19** is a true transition structure with one imaginary frequency of -305 cm^{-1}. It thus appears that the high energy minimum found with the "static" solvation model is a consequence of insufficient geometrical relaxation. For the most part, however, the potential energy curves of the "relaxed" and the "static" solvation model are very similar, indicating that little structural relaxation occurs through solvation along most parts of the reaction coordinate. This result also points to the fact that water−solute interactions are mainly electrostatic in nature and approximately additive in this system. The "relaxed" solvent model also has its insufficiencies, as the water molecules cannot be kept in pairs along the reaction path. When the system progresses beyond values of 1.2 on the reaction coordinate, a major reorientation of the four water molecules leads to a drastic lowering of the potential energy. The structure obtained after full relaxation **21** has all four water molecules aligned in a half circle through hydrogen bonds, with the ethylene radical cation attached to one of the terminal water molecules. The energy gained during this reorientation step is mainly due to changes in water−water interactions and thus is not indicative of radical cation solvation.

A third approach toward estimating solvation effects along reaction coordinates consists in combining gas phase *ab initio* potential energies with differences of free energy of solvation obtained from empirical Monte Carlo solution simulations.[15] This procedure has provided valuable insights into solvation effects in nucleophilic substitution reactions of closed shell[16] and open shell[12,13] systems. In the simulation, the interaction energy between solute molecule x and solvent molecule y is given by a combination of Coulomb and Lennard-Jones terms as in eq 1.

$$\Delta E_{xy} = \sum_i \sum_j \left[\frac{q_i q_j e^2}{r_{ij}} + 4\epsilon_{ij} \left\{ \left(\frac{\sigma_{ij}}{r_{ij}} \right)^{12} - \left(\frac{\sigma_{ij}}{r_{ij}} \right)^{6} \right\} \right] \qquad (1)$$

The summation runs over all i interaction sites on solute x and j interaction sites on solvent molecule y. The interaction sites have been chosen identical to the locations of atoms in the solutes in this study.

Gas phase structures for **14**, **17**, and a number of connecting points can only be used for the MC solution simulations if no major structural changes occur upon solvation. As noted before, only small changes are observed for structure **17** when two additional water molecules are added such as in **20**. It therefore appears that specific solvent effects will have only a minor influence on the structure of **17**. Solvation effects of bulk solvent can be modeled with continuum models such as the Onsager self-consistent reaction field (SCRF) model. Unfortunately, geometry optimizations are not possible with UMP2 wave functions together with the SCRF solvent model. In order to investigate solvent induced geometrical changes of the

(15) (a) Jorgensen, W. L. *Acc. Chem. Res.* **1989**, *22*, 184. (b) Kollman, P. *Chem. Rev.* **1993**, *93*, 2395.

(16) (a) Chandrasekhar, J.; Smith, S. F.; Jorgensen, W. L. *J. Am. Chem. Soc.* **1985**, *107*, 154. (b) Chandrasekhar, J.; Jorgensen, W. L. *J. Am. Chem. Soc.* **1985**, *107*, 2974.

Table 2. Absolute and Relative Energies and Zero Point Vibrational Energies for Stationary Points on the 2*Water + Ethylene Radical Cation and the 4*Water + Ethylene Radical Cation Potential Energy Surface[g]

	E_{tot}[a]							
structure	(PMP2/6-31G*)	(PMP2/6-311+G**)	(PMP4/6-311+G**)	ZPE[b]	NIMAG[c]	ΔE_1[d]	ΔE_2[e]	ΔE_3[f]
9	−230.41133	−230.60258	−230.66394	65.3	0	=0.0	=0.0	=0.0
1 + 3	−230.36425	−230.55992	−230.62206	63.4	0	+29.5	+24.9	+24.3
2 + 12	−230.32384	−230.52510	−230.58799	60.7	0	+54.9	+44.0	+43.1
10 + 11	−230.33420	−230.52833	−230.58993	63.8	0	+48.4	+45.1	+44.9
13	−230.38263	−230.57674	−230.63889	64.5	1	+18.0	+15.4	+14.9
14	−230.38320	−230.57724	−230.63942	64.6	0	+17.7	+15.2	+14.7
15	−230.38357			64.7	0	+17.4		
16	−230.38307			64.5	0	+17.7		
17	−230.37680	−230.57272	−230.63644	62.9	1	+21.7	+16.3	+14.9
18	−230.37564	−230.57207	−230.63565	63.2	0	+22.4	+17.0	+15.6
19	−230.36525	−230.56316	−230.62605	62.2	0	+28.9	+21.6	+20.6
20	−382.82359			95.4	1	+26.3		
21	−382.86551					=0.0		

[a] UMP2/6-31G* optimized geometries. [b] Unscaled UMP2/6-31G* vibrational frequencies. [c] Number of imaginary frequencies. [d] PMP2/6-31G*//UMP2/6-31G* energies. [e] PMP2/6-311+G**//UMP2/6-31G* energies + ΔZPE(UMP2/6-31G*). [f] PMP4/6-311+G**//UMP2/6-31G* energies + ΔZPE(UMP2/6-31G*). [g] Absolute energies are in hartrees and relative energies in kcal/mol.

Table 3. Lennard-Jones Parameters for the Monte Carlo Solution Simulations Along the **14** → **17** Reaction Coordinate

atom	σ [Å]	ϵ [kcal/mol]
C	2.50	0.066
O	3.23	0.174
H(CH_2)	2.20	0.030
H(OH_2)	0	0

substrate, the structure of **17** was reoptimized at the UHF/6-31G* level of theory, once in the gas phase and once in the presence of the reaction field, using a cavity radius of 3.59 Å and a continuum dielectric constant of $\epsilon = 78$. The UHF/6-31G* structure of **17** has longer C−O distances (2.377 Å) and a slightly shorter C−C bond (1.4047) as compared to the UMP2/6-31G* structure (Figure 5). Inclusion of the SCRF model increases this trend slightly and leads to C−O distances of 2.3944 Å and a C−C distance of 1.4041 Å. Calculation of ESP charges for both the gas phase and the SCRF UHF/6-31G* geometries gives very similar results. Since neither specific nor unspecific solvent effects appear to have a significant influence on the structure and the charge distribution of **17**, gas phase UMP2/6-31G* structures have been used without modification for all solution simulations.

Coulomb parameters were obtained for all UMP2/6-31G* optimized gas phase structures by fitting the *ab initio* molecular electrostatic potential to point charges (ESP charges) for each point along the reaction coordinate between **14** and **17**.[17] Lennard-Jones parameters were initially chosen from structurally similar molecules from the literature.[18,19] They were then modified such that the OPLS model reproduces the *ab initio* structures of water−solute complexes (Table 3). The final values used for the ethylene radical cation carbon atoms are rather close to those employed in solution simulations of the *tert*-butyl cation.[18] Since solute−solvent effects are dominated by Coulomb interactions for this charged solute, the same Lennard-Jones parameters have been used for all structures along the reaction coordinate. The interaction energies calculated with this initial parameter set (termed "OPLS_I") for complexes of one TIP4P water molecule and eight structures along the reaction coordinate between **14** and **17** are substantially lower as compared to UHF/6-31G* energies (Figure 9, open boxes). To increase the monosolvation energies in a systematic way, the

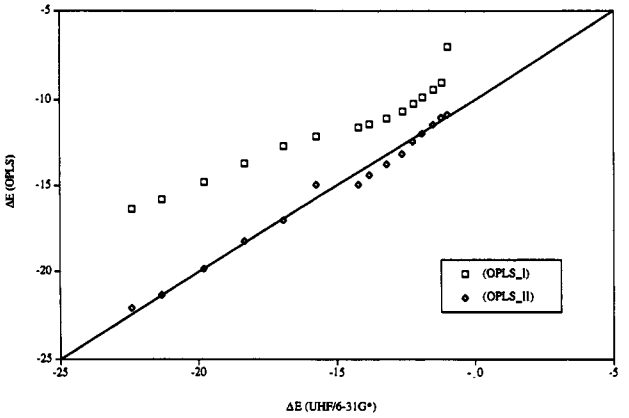

Figure 9. Correlation of monosolvation energies calculated with the OPLS models I and II with *ab initio* UHF/6-31G* values.

ESP-derived solute point charges[17] were scaled by a factor of 1.35 relative to the average charge of +0.083e. This leads to increased intramolecular charge separation within the solutes as well as enhanced monosolvation energies as shown in Figure 9 (open diamonds). Monte Carlo solution simulations were then performed with both parameter sets to determine, in how far the results of the simulations depend markedly on the choice of potential parameters. A cubic box containing one solute and 263 TIP4P water molecules has been employed at 298 K and 1 atm. The free energy of solvation changes on going from **14** to **17** have been calculated in 17 windows using the double wide sampling technique.[20] For each window, the system was equilibrated for 10^6 MC steps, followed by 4×10^6 steps of averaging in the NPT ensemble. This number was sufficient to keep the standard deviation for each window below 10% of the corresponding free energy change. The resulting partial free energy profiles shown result from the combination of the *ab initio* gas phase potential energies with changes in free energy of solvation from MC simulations (Figure 10). Monte Carlo standard deviation bars have been included. Simulations with both parameter sets predict transition structure **17** to be less well solvated as compared to complex **14** by 5.0 kcal/mol (OPLS_I) or 8.3 kcal/mol (OPLS_II). Also, both parameter sets predict the free energy profile to be rather flat in the vicinity of the transition structure, parameter set OPLS_II giving a somewhat more rugged PMF curve.

Considering the very different nature of solvation models, it is quite surprising that the inclusion of single solvating water

(17) Breneman, C. M.; Wiberg, K. B. *J. Comput. Chem.* **1990**, *11*, 431.
(18) Jorgensen, W. L.; Buckner, J. K.; Huston, S. E.; Rossky, P. J. *J. Am. Chem. Soc.* **1987**, *109*, 1891.
(19) Jorgensen, W. L.; Chandrasekhar, J.; Madura, J. D.; Impey, R. W.; Klein, M. L. *J. Chem. Phys.* **1983**, *79*, 926.
(20) Jorgensen, W. L.; Ravimohan, C. *J. Chem. Phys.* **1985**, *83*, 3050.

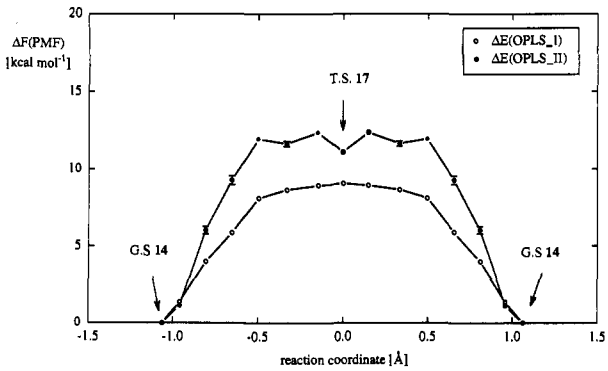

Figure 10. Solvent effects on the $S_{RN}2$-interconversion barrier from Monte Carlo solution simulations with two different parameter sets OPLS_I and OPLS_II (see text).

Scheme 2

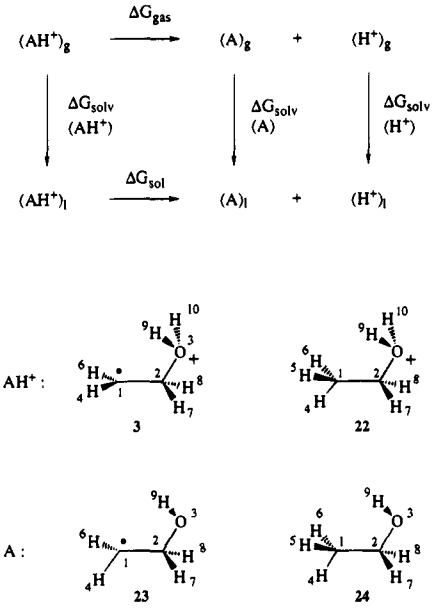

molecules in the *ab initio* studies yield very similar effects as compared to solution simulations with a large number of water molecules (Figure 7 vs Figure 10). One feels tempted to conclude, that attaching one solvating water molecule each to both substrate water molecules in complex **14** captures the essence of aqueous solvation. With various solvation models predicting transition structure **17** to be less well solvated as compared to complex **14**, one must also conclude that solvent effects *alone* are unlikely to turn gas phase transition states for $S_{RN}2$ substitution into symmetrically bridged solution phase minima.

4.b. Acidity of Distonic Ions. The second remarkable feature of the potential energy surface shown in Figure 4 besides the low barriers for $S_{RN}2$- and $S_{RN}2'$-reactions is the low acidity of distonic ion **3**. Characterization of the acidity of **3** as "low" is based, of course, on the comparison of deprotonation with other possible reaction paths. Also, solvation effects might considerably alter the gas phase acidity. Of much larger value for the interpretation of experimental data would therefore be the calculation of the pK_a for distonic ion **3** in aqueous solution. This value can be calculated indirectly by using the thermochemical cycle shown in Scheme 2 and eq 2

$$2.3RT\mathrm{p}K_a(\mathrm{AH}^+) = \Delta G_{sol}(\mathrm{AH}^+) = -\Delta G_{solv}(\mathrm{AH}^+) + \Delta G_{gas}(\mathrm{AH}^+) + \Delta G_{solv}(\mathrm{A}) + \Delta G_{solv}(\mathrm{H_3O}^+) \quad (2)$$

Using eq 2 for distonic ion **3** and for protonated ethanol (**22**) allows the expression of the pK_a of **3** in terms of free energy of solvation *differences* for these two cations in their protonated and deprotonated states and the pK_a for protonated ethanol as given in eq 3.[21] The pK_a of protonated ethanol has been determined recently by ^{13}C-NMR measurements.[22]

$$2.3RT[\mathrm{p}K_a(\mathbf{3}) - \mathrm{p}K_a(\mathbf{22})] = = \Delta\Delta G_{gas}(\mathbf{3}-\mathbf{22}) + \Delta\Delta G_{solv}[(\mathbf{23})-(\mathbf{24})] - \Delta\Delta G_{solv}(\mathbf{3}-\mathbf{22}) \quad (3)$$

Calculation of the difference in gas phase free energy of deprotonation between **3** and **22** $\Delta\Delta G_{gas}(\mathbf{3}-\mathbf{22})$ was based on the PMP4/6-311+G**//UMP2/6-31G* relative energy of −0.32 kcal/mol, which changes slightly to +0.2 kcal/mol after inclusion of the difference in UMP2/6-31G* zero point energy. The vibrational frequencies were then used to calculate enthalpy and entropy contributions to the free energy difference at 298 K.[21] Overall, a value of $\Delta\Delta G_{gas}(\mathbf{3}-\mathbf{22}) = -0.31$ kcal/mol is obtained from these calculations, making the acidity of distonic ion **3** and of protonated ethanol comparable. Larger differences in solution phase acidities must therefore arise from differential solvation effects. These solvent effects are composed of two factors, the free energy of solvation difference between the deprotonated forms **23** and **24** and that between the ions **3** and **22**. These components have again been estimated with Monte Carlo free energy perturbation calculations.

To calculate $\Delta\Delta G_{solv}[(\mathbf{23})-(\mathbf{24})]$, various conformations have been optimized for ethanol (**24**) and for the ethanol-2-yl radical (**23**) at the UMP2/6-31G* level of theory. The most favorable gas phase geometries used in the perturbation calculations are those shown in Scheme 2. Lennard-Jones parameters were chosen from literature values for alcohols and are given in Table 4. Coulomb parameters were obtained by fitting the UMP2/6-31G* electrostatic potential to point charges located at atomic positions. Since ESP derived charges depend on molecular conformation,[23] different charges were obtained for various conformers of **23** and **24** and Boltzmann-averaged values for the two most favorable conformations have been used (Table 4). The perturbation from **23** to **24** was performed in ten steps using the double wide sampling procedure. A cubic box containing 264 TIP4P water molecules was used at 25 °C and 1 atm. Each window required 1 M steps of equilibration followed by 4 M steps of averaging. The final value obtained for $\Delta\Delta G_{H_2O}[(\mathbf{23})-(\mathbf{24})]$ with this procedure is -0.85 ± 0.05 kcal/mol. Ethanol (**24**) is therefore slightly better solvated in water than the ethanol-2-yl radical **23**. Conducting the same perturbation calculation in acetonitrile with 265 solvent molecules per box at 25 °C and 1 atm gives an almost identical value of $\Delta\Delta G_{CH_3CN}[(\mathbf{23})-(\mathbf{24})] = -0.99 \pm 0.02$ kcal/mol.

Much larger solvent effects should be expected for the protonated forms, even though the interest here is in *relative* free energies of solvation and not absolute values. Lennard-Jones parameters for the OPLS representation of **3** and **22** have been chosen again from the literature and Coulomb parameters have been obtained from fitting the MP2/6-31G* electrostatic potential. ESP-derived charges represent averages over the two most favorable conformers for both **3** and **22** (Table 4). The perturbation from **3** to **22** was performed as before and a final

(21) Jorgensen, W. L.; Briggs, J. M. *J. Am. Chem. Soc.* **1989**, *111*, 4190.
(22) Donald, G. L.; Demchuk, K. J. *Can. J. Chem.* **1987**, *65*, 1769.
(23) (a) Essex, J. W.; Reynolds, C. A.; Richards, W. G. *J. Am. Chem. Soc.* **1992**, *114*, 3634. (b) Reynolds, C. A.; Essex, J. W.; Richards, W. G. *J. Am. Chem. Soc.* **1992**, *114*, 9075. (c) Reynolds, C. A.; Essex, J. W.; Richards, W. G. *Chem. Phys. Lett.* **1992**, *199*, 257. (d) Williams, D. E. *Biopolymers* **1990**, *29*, 1367. (e) Cornell, W.; Cieplak, P.; Bayly, C.; Kollman, P. A. *J. Am. Chem. Soc.* **1993**, *115*, 9620.

Table 4. Lennard-Jones and Coulomb Parameters for Monte-Carlo Solution Simulations for the Ethanol-2-yl Radical **23** and for Ethanol **24**

	parameters for **23/24**				parameters for **3/22**			
center	σ [Å]	ϵ [kcal/mol]	q(**24**) [e^{-1}]	q(**23**) [e^{-1}]	σ [Å]	ϵ [kcal/mol]	q(**3**) [e^{-1}]	q(**22**) [e^{-1}]
C1	3.50	0.066	−0.243	−0.384	3.50	0.066	−0.303	−0.371
C2	3.50	0.066	+0.404	+0.442	3.50	0.066	0.284	0.254
O3	3.08	0.174	−0.672	−0.665	3.08	0.174	−0.576	−0.562
H4	2.50	0.030	+0.042	+0.115	2.50	0.030	0.185	0.165
H5	2.50	0.030	+0.069		2.50	0.030		0.137
H6	2.50	0.030	+0.074	+0.135	2.50	0.030	0.185	0.137
H7	2.50	0.030	−0.018	−0.050	2.50	0.030	0.116	0.110
H8	2.50	0.030	−0.056	+0.011	2.50	0.030	0.116	0.110
H9	0.00	0.000	+0.400	+0.396	0.00	0.00	0.497	0.510
H10					0.00	0.00	0.497	0.510

value for $\Delta\Delta G_{solv}$[(**3**)−(**22**)] of −1.87 ± 0.04 in water and −1.45 ± 0.03 in acetonitrile has been calculated. This result shows that distonic ion **3** is less well solvated in aqueous as well as acetonitrile solution due to larger charge delocalization as compared to its closed shell counterpart **22**.

Using eq 3, the predicted pK_a difference between **3** and **22** then amounts to $\Delta pK_a = +0.52$ in water and $\Delta pK_a = +0.15$ in acetonitrile. Distonic ion **3** is therefore predicted to be slightly less acidic as compared to protonated ethanol. With the measured pK_a for protonated ethanol of pK_a = −3.67, the predicted value for distonic ion is pK_a(**3**) = −3.15 at 298 K. This makes distonic ion **3** a thermodynamically highly acidic species in aqueous solution in comparison to other organic acids and highlights the importance of including solvent effects in calculations of acidities.

5. A Larger Model System—*trans*-Butene Radical Cation + Water

The choice of this model system is motivated by the fact that most alkenes used in electron transfer catalysis contain at least one but usually two or three substituents at the carbon−carbon double bond. Most of these substituents will lower the alkene ionization potential by stabilization of the alkene radical cation. Based on the findings in the ethylene + water system, one would then have to expect the water addition of substituted alkene radical cations to be less thermodynamically favorable. This has indeed been shown by an early model study, in which the reactions of water with propene and enol ether radical cations have been investigated at the UHF/4-31G//UHF/STO-3G level of theory.[7] Another finding of this study was the preference of bridged structures in substituted alkene radical cation−water adducts. For the *trans*-2-butene radical cation (**25**), the stabilizing effect of the two methyl groups can be estimated by isodesmic eq 4, which includes nothing else but the difference in adiabatic ionization potentials of ethylene and *trans*-butene.

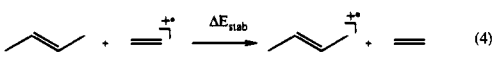

(4)

Using experimentally determined gas phase heats of formation, ΔE_{stab} amounts to −31.9 kcal/mol.[24] Theoretical values based on PMP2/6-311+G**//UMP2/6-31G* + ΔZPE(UMP2/6-31G*) energies yield −29.0 kcal/mol, those based on PMP4/6-311+G**//UMP2/6-31G* + ΔZPE(UMP2/6-31G*) energies give −29.6 kcal/mol. Thus, experimentally as well as theoretically deduced data unequivocally show significant stabilization of alkene radical cations by alkyl substituents. That alkene radical cation stabilization according to eq 4 also leads to reduced reactivity is reflected in the much smaller exothermicity

(24) Lias, S. G.; Liebman, J. F.; Vevin, R. D.; Kafafi, S. A. *NIST Standard Reference Database, Positive Ion Energetics*; Version 2.01, Jan 1994.

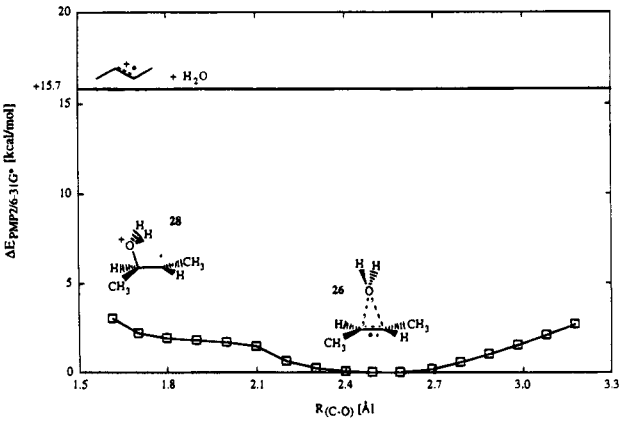

Figure 11. Potential energy curve for water addition to the *trans*-2-butene radical cation at the PMP2/6-31G* level of theory.

for water addition to *trans*-2-butene as compared to ethylene radical cation (Figure 11). While addition of water to ethylene is exothermic by −32.7 kcal/mol at the PMP2/6-31G* level of theory, this value is reduced to −15.7 kcal/mol for the addition of water to *trans*-2-butene radical cation. Morover, the butene−water adduct does not share the distonic ion structure with water adduct **3** but rather closely resembles transition structure **4**, in which the water molecule is placed symmetrically over the alkene C−C bond. The closest distance between alkene radical cation carbon and water oxygen in **26** is 2.493 Å, slightly longer than the value of 2.364 found in **4**. The water molecule in **26** is not placed perfectly symmetrical over the *trans*-butene radical cation. Energetically as well as geometrically, however, the difference to the fully C_2 symmetric structure **27** with carbon−oxygen bond distances of 2.585 Å is rather small (Table 1). Starting from **28** and elongating the C−O bond distance, again no transition structure could be found. One has to conclude then on energetic as well as structural grounds that the addition of two methyl groups to the ethylene radical cation prevents the formation of distonic ions of type **3** and instead only allows formation of ion−dipole complexes. By artificially restricting the C−O bond length in **26** to shorter values, one can also estimate, how much energy separates a hypothetical distonic ion structure from complex **26**. Restriction of the C−O bond length to a value of 1.614 Å as in distonic ion **3** and relaxation of all other geometrical variables leads to structure **28**, which is located +3.0 kcal/mol above **26** at the PMP2/6-31G* level of theory. Considering the large geometrical changes involved on going from **26** to **28** (Figure 12), this small energy difference is quite surprising! Of course, it must be remembered that **28** is located +3.0 kcal/mol *above* complex **26** while **3** is located −10.3 kcal/mol *below* complex **4** at the PMP2/6-31G* level of theory. Overall, the inclusion of two methyl groups therefore destabilizes distonic ion formation by ca. 13 kcal/mol. That is, again, a much smaller value as compared to the isodesmic

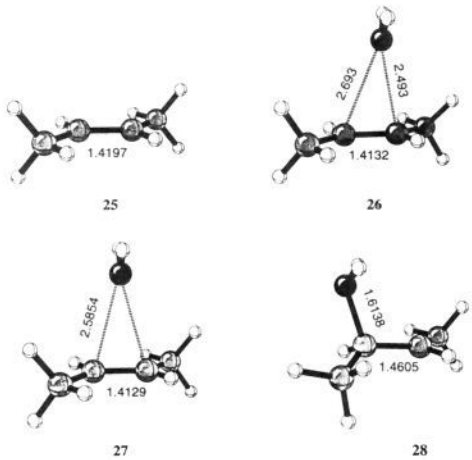

Figure 12. UMP2/6-31G* optimized geometries of selected points in the water + *trans*-2-butene radical cation system.

Scheme 3

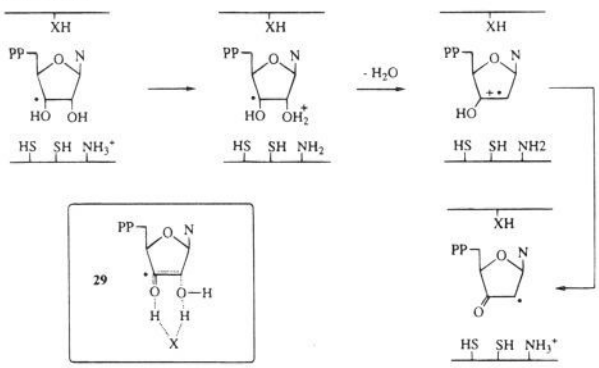

energy obtained from eq 4. This fact can well be explained by assuming that, whatever effects are responsible for isodesmic stabilization of alkene radical cations, the same effects must still be partially active after formation of distonic ions.

To what extent are these conclusions also significant for reactions of alkene radical cations in solution? Certainly, the stabilization of distonic ion structures by solvent molecules as found in the small model system will also be effective in reactions of larger alkene radical cations. In contrast to the reaction of ethylene radical cation, however, significant solvent support is now necessary not only for the deprotonation step but also for distonic ion formation. Experimentally, this should manifest itself by large solvent effects in reactions of alkene radical cations with weak nucleophiles such as water.

The reluctance of the *trans*-butene radical cation to form distonic ions with water also has some implications for the ribonucleotide reductase mechanism. This enzyme catalyzes the C2′-reduction of ribonucleotides to the corresponding desoxy-analogs.[25] The proposed catalytic reaction mechanism includes radical formation at the C3′ carbon atom of the ribose ring and removal of the C2′ hydroxy group through a protonation/elimination sequence under concomitant 1,2-shift of the radical center (Scheme 3). It is in this latter step that a distonic ion is commonly assumed to occur before elimination. Based on the results obtained in this study for the butene radical cation, it appears rather unlikely that the assumed distonic ion exists as an intermediate in the ribonucleotide reductase mechanism. The alkene radical cation formed after water elimination is not only stabilized by two ring methylene groups but also by one hydroxy substituent, which must be expected to be even more stabilizing as compared to alkyl groups. The expected larger stabilization of the radical cation makes formation of a distonic radical cation through water addition altogether very unlikely, unless this ion is stabilized through the enzyme binding pocket. But why should this be advantageous for enzyme catalytic efficiency? It is much more likely that protonation and water elimination occur in concert without intermediate formation of any distonic species. Based on the drastically lower barriers found for substitution[12,13] as well as elimination[26] reactions in open shell species, a second mechanistic scenario seems possible. The overall elimination of one molecule of water from the ribose moiety can in principle also be achieved by binding of the substrate such that some group XH connects the ribose C2′ and C3′ hydroxy groups. If the radical is then formed by C3′ hydrogen abstraction, the 1,3-elimination of water should occur readily with a very small barrier and in a concerted manner as shown in structure **29**. Model studies to evaluate this possibility are in progress.

(25) Stubbe, J. *J. Biol. Chem.* **1990**, *265*, 5329.

Conclusion

From the investigation of the water + ethylene radical cation and the water + *trans*-butene radical cation systems one must conclude that the reactivity of alkene radical cations is dominated by thermodynamic effects. No gas phase potential energy barrier has been found for addition of water to either of the two alkene radical cations. Addition leads to the formation of distonic radical cations only if the alkene radical cation is not stabilized by electron donating substituents such as alkyl groups. Water molecules bound in distonic radical cations can easily be exchanged by other nucleophiles such as additional water molecules. This exchange can proceed either through an $S_{RN}2$-type pathway or through a novel $S_{RN}2'$-type process involving addition of the nucleophile to the radical center. The influence of solvation on the substitution barrier has been studied in various ways and has been shown to increase the gas phase substitution barrier approximately twofold in water. The acidity of distonic radical cations is drastically influenced by solvation effects. While proton transfer from the ethylene radical cation derived distonic ion to water is a highly unfavorable process in the gas phase, solvent effects transform the distonic ion into a highly acidic species in aqueous solution. No distonic ion formation is found for the reaction of water with *trans*-butene radical cation. Instead, an ion−dipole complex is formed in the gas phase.

Acknowledgment. This study was supported by the Deutsche Forschungsgemeinschaft and the Fonds der Chemischen Industrie through a Liebig Stipendium. Thanks are also due to Prof. H. Schwarz (TU Berlin) for constant encouragement and generous support and to Prof. B. Giese (Basel) and Prof. S. Shaik (Hebrew University of Jerusalem) for helpful discussion. Computational resources were provided by the Zentraleinrichtung Rechenzentrum TU Berlin and by the Konrad-Zuse-Zentrum für Informationstechnik Berlin.

Supporting Information Available: Structures of optimized stationary points (8 pages). This material is contained in many libraries on microfiche, immediately follows this article in the microfilm version of the journal, can be ordered from the ACS, and can be downloaded from the Internet; see any current masthead page for ordering information and Internet access instructions.

JA952019L

(26) Zipse, H. Unpublished results.

(27) (a) Wong, M. W.; Frisch, M. J.; Wiberg, K. B. *J. Am. Chem. Soc.* **1991**, *113*, 4776. (b) Wong, M. W.; Wiberg, K. B.; Frisch, M. *J. Chem. Phys.* **1991**, *95*, 8991.